

# Grating-based X-ray dark-field imaging: a new paradigm in radiography

Andre Yaroshenko · Katharina Hellbach ·  
Martin Bech · Susanne Grandl · Maximilian F. Reiser ·  
Franz Pfeiffer · Felix G. Meinel

Published online: 23 May 2014  
© Springer Science+Business Media New York 2014

**Abstract** Grating-based X-ray dark-field contrast is an emerging new imaging modality that is demonstrating particularly high potential for radiography. The signal in dark-field X-ray imaging is determined by small-angle X-ray scattering at structures typically below the spatial resolution of the imaging setup. Thus, this technique not only yields complementary information but also visualizes information that lies under the resolution limit for conventional, absorption-based radiography. Grating-based X-ray dark-field imaging has been shown to be feasible with both synchrotron radiation and conventional X-ray tubes. Lung, breast, and bone imaging have been identified as the applications promising the main impact, but other applications are on the horizon. Specifically, dark-field radiography has been used to detect pulmonary emphysema and assesses its regional distribution in mice and holds promise to improve the visualization of micro-calcifications in mammography and yields information about bone microstructure. Further technical developments are required to make the technique suitable for clinical use.

**Keywords** X-ray phase-contrast imaging · X-ray dark-field imaging · Grating-based imaging · Grating interferometry, Lung imaging · Pulmonary emphysema

## Introduction

Clinical X-ray imaging, so far, depends solely on the X-ray absorbing properties of tissues and materials. Since the X-ray attenuation coefficient is roughly proportional to the fourth power of the atomic number  $Z$  [1] tissues composed of heavier atoms (e.g., bones and teeth) show a high contrast on conventional X-ray images. Soft tissue, mainly composed of light elements, yields only low contrast. X-ray phase-sensitive imaging methods have the potential to not only overcome the limitation of low soft tissue contrast but also visualize biophysical tissue properties that are inaccessible for conventional radiography. These imaging methods, similar to the concepts known from light microscopy [2], use the wave nature of X-rays. Passing through matter, X-rays not only get absorbed but are also refracted, i.e., are deviated from their original propagation direction by a certain angle. Measurement of the deviation angle yields complementary information in comparison to the conventional attenuation-based imaging. Different approaches make it possible to acquire X-ray phase information [3–7] and have been in use at large scale synchrotron facilities since the first groundbreaking experiments reported by Bonse and Hart in 1965 [8]. However, only in 2006, the Talbot-Lau X-ray interferometer has been reported [9, 10] which allows to acquire X-ray phase information with conventional polychromatic laboratory sources. Since then, considerable efforts have been devoted to applying this method to different biomedical applications. The present review presents an

---

This article is part of Topical Collection on *New Imaging Technologies*.

---

A. Yaroshenko · F. Pfeiffer  
Lehrstuhl für Biomedizinische Physik, Physik-Department &  
Institut für Medizintechnik, Technische Universität München,  
James-Frank Str. 1, 85748 Garching, Germany

K. Hellbach · S. Grandl · M. F. Reiser · F. G. Meinel (✉)  
Institute for Clinical Radiology, Ludwig-Maximilians-University  
Hospital Munich, Marchioninstr. 15, 81377 Munich, Germany  
e-mail: felix.meinel@med.uni-muenchen.de

M. Bech  
Medical Radiation Physics, Lund University, Barngatan 2:1,  
22185 Lund, Sweden

overview over the physical principles of dark-field radiography as well as recent results of experiments applying the technique to biomedical imaging.

### Physical and Technical Principles of Grating-Based X-Ray Dark-Field Imaging

Currently, the most spread method for obtaining X-ray phase information with conventional laboratory sources is based on the use of a three-grating Talbot-Lau interferometer. This method utilizes three gratings between the X-ray source and detector. The first (absorption) grating, a so-called source grating, is placed as close as possible to the X-rays source emission point and divides the source into a number of line sources, thus creating spatial coherence in the beam. A certain distance downstream of the source grating a phase grating is placed. It gives rise to an interference pattern (i.e., typically a combination of dark and light stripes) further downstream. This interference pattern is registered with and without the sample in the beam, and deviations in the pattern reveal phase information. However, since the interference pattern is typically too small to be directly resolved by clinically used detectors, the third grating (a so-called analyzer grating) is placed just in front of the detector. This last absorption grating is moved in a number of steps perpendicular to the beam propagation direction and grating lamellae over one grating period, acquiring a detector image for each new grating position. Thus, a so-called intensity stepping curve [11] is acquired, which gives the registered intensity in a pixel as a function of the analyzer grating position. This way, information about the interference pattern can be obtained, without directly resolving it. By comparing the stepping curves acquired with and without the sample, it is possible to calculate conventional transmission, differential phase-contrast, and dark-field images if the stepping was performed with at least three steps [12]. Thus, three image contrasts can be obtained simultaneously, and the images can be directly compared pixel by pixel.

In particular, conventional transmission is obtained as the mean value of the stepping curve performed with the sample, normalized by the corresponding value acquired without the sample. Differential phase-contrast is calculated as the shift of the stepping curve, acquired with the sample, compared to the reference curve. And the dark-field contrast is obtained as the amplitude of the stepping curve with the sample divided by the amplitude without the sample and normalized by the transmission signal [9–11].

The three imaging signals originate from different physical processes. While conventional transmission reveals the amount of photons absorbed in the sample, the differential phase-contrast gives the first derivative of the

wave phase shift caused by the sample. If the phase shift is too small to be directly resolved by the grating interferometer, a dark-field signal is generated. The origin of the dark-field can be considered as small-angle scattering, which leads to a damping of the amplitude of the stepping curve. Hence, the dark-field can visualize structures that are smaller than the resolution of the system. This way, for example, the alveoli in the lung can be clearly visualized in dark-field radiography.

To avoid the differential depiction, the phase shift information can be derived from the differential phase-contrast signal by integration. Different methods [13, 14] for noise reduction integration algorithms have been reported both for projection and tomographic acquisitions. However, their application to radiographs remains challenging.

A further grating-based approach used to retrieve phase information with conventional polychromatic laboratory sources is based on the introduction of a periodic illumination pattern on the detector that can be directly resolved. Typically, a simple absorption grating is illuminated to produce such a pattern [15, 16]. Alternatively, the interference pattern can be achieved by introducing Moiré fringes on the detector through slightly tilted gratings or a different structure [17, 18].

To retrieve the three imaging modalities, a radiographic image is acquired with and without the sample in the beam. The images are subsequently considered in Fourier space. Due to the introduced pattern on the detector, two distinct peaks are obtained in Fourier space, corresponding to the 0th and the 1st Fourier component. A mask is applied in Fourier space to take the 0th order or the 1st order peak, respectively. Subsequently, the information is transformed back to the real space. This approach allows obtaining transmission as well as phase-contrast and dark-field images. Although this method is relatively easy to realize experimentally, it suffers from significantly lower sensitivity than the approach with the three-grating interferometer.

### Lung Imaging

Ex vivo [19, 20], in situ [21], and in vivo [22] studies in mice have shown that healthy lung tissue generates a very strong dark-field signal generated by small-angle X-ray scattering at the multiple air-tissue interfaces that characterize the micro-architecture of normal pulmonary parenchyma. Indeed, in whole-body radiographs of mice, the lungs stand out as the single organ that generates by far the strongest dark-field signal (Fig. 1) [22]. Focal or diffuse pulmonary pathologies alter the pulmonary parenchymal architecture. This often leads to a decrease in the genuinely strong dark-field signal from lung tissue, and pulmonary pathologies can thus be detected on dark-field radiographs.

**Fig. 1** Whole body radiograph of a healthy mouse in vivo. Transmission (a) and dark-field (b) images are shown illustrating that transmission and dark-field radiographs visualize different biophysical properties. Tissues with multiple air-tissue interfaces such as lungs and fur generate small-angle X-ray scattering visible as the dark-field signal [22••]



For this reason, lung imaging is arguably the most promising biomedical application for X-ray dark-field imaging at the moment.

### Pulmonary Emphysema

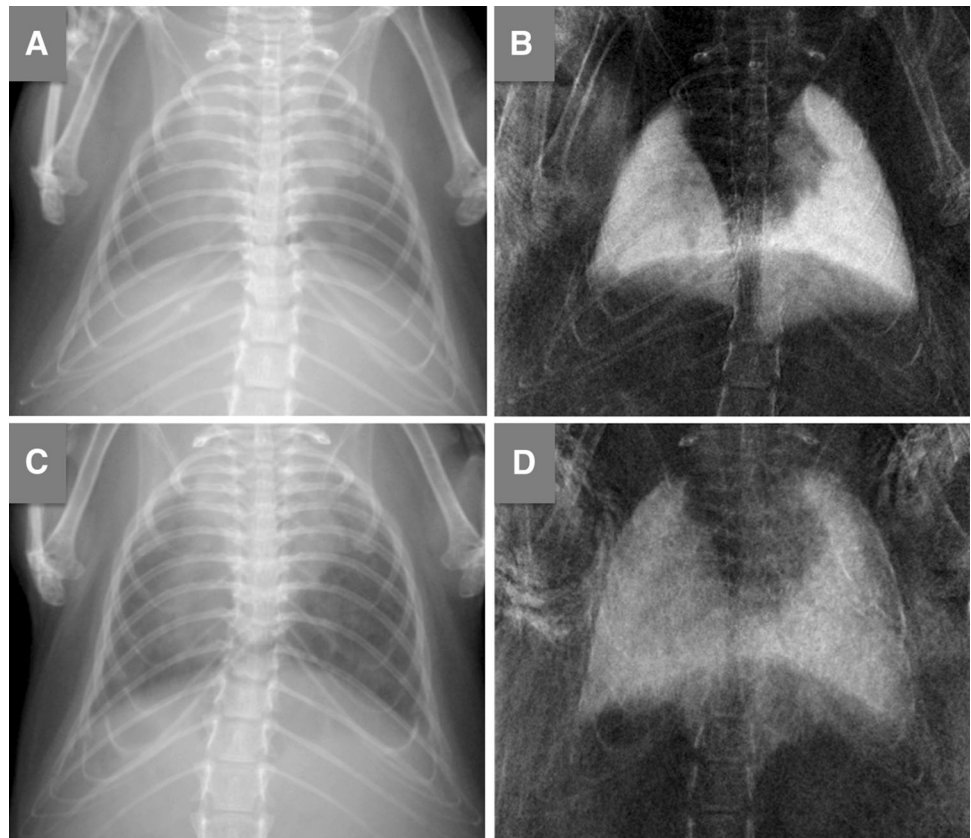
Pulmonary emphysema is commonly associated with chronic obstructive lung disease and thus most commonly seen in patients with a history of smoking. If detected early, the progression of pulmonary emphysema can be delayed by smoking cessation. Interventional techniques such as bronchial valves or lung volume reduction surgery can relieve symptoms by removing or decreasing ventilation to lung parenchyma with advanced destruction. Lung transplantation remains the only curative treatment, but this procedure is associated with high mortality and morbidity and is thus only suitable for a minority of patients with end-stage pulmonary emphysema.

The diagnosis and severity assessment of pulmonary emphysema on chest radiographs is challenging, particularly in the early stages of the disease. Conventional chest radiographs can only visualize indirect signs of the increased pulmonary volume seen in emphysema such as a flattened diaphragm, widely spaced ribs as well as increased chest diameter and increased retrosternal air space on the lateral view. Consequently, chest radiographs have been shown to be reasonably accurate for advanced

emphysema but only moderately sensitive in mild to moderate emphysema with substantial inter-observer variability [23–26].

The feasibility of visualizing pulmonary emphysema with dark-field imaging was first demonstrated using a near-monochromatic high-flux X-ray source [19••]. The study used excised murine lungs derived from a murine model of elastase-induced pulmonary emphysema and control mice and demonstrated that the dark-field signal can be used to discriminate healthy and emphysematous lungs and to map the distribution of emphysema on radiographs [19••]. Another publication based on the same data set showed that dark-field signal provides incremental diagnostic value compared to the transmission signal for detecting pulmonary emphysema and assessing its regional distribution [27•]. The combination of dark-field and transmission images can be used to normalize the dark-field signal over the transmission signal and thus derive a parameter that represents the local small-angle scattering power of the tissue sample independent of its thickness and is often referred to as “normalized scatter”. It has been shown that the analysis of normalized scatter—and thus the combination of dark-field and transmission imaging—has even higher discriminatory power for the detection of pulmonary emphysema than dark-field imaging alone [19••, 27•]. These initial studies had been performed with a laser-driven X-ray source that resembles a synchrotron in its

**Fig. 2** Visualization of pulmonary emphysema in vivo. Transmission (**a, c**) and dark-field (**b, d**) images of a healthy mouse lung (*upper row*) and an emphysematous lung (*lower row*) are shown. Only indirect signs of increased intrathoracic volume are visible in the transmission images. In contrast, the marked difference in dark-field signal intensity directly visualizes the changes in lung microarchitecture [30••]



X-ray beam properties [19••]. More recently, it has been shown that the detection and mapping of pulmonary emphysema with grating-based X-ray imaging can be successfully performed using a conventional polychromatic X-ray tube [28••]. The X-ray source was integrated into a prototype small-animal dark-field X-ray scanner, which can be operated in a normal laboratory environment [29]. This represents a major step toward a potential clinical applicability of the technique, since the installation of mono-energetic X-ray sources would hardly be feasible in a clinical setting. Using the same experimental set-up, dark-field imaging of pulmonary emphysema has been successfully performed in vivo in anesthetized, freely breathing mice (Fig. 2) [30••].

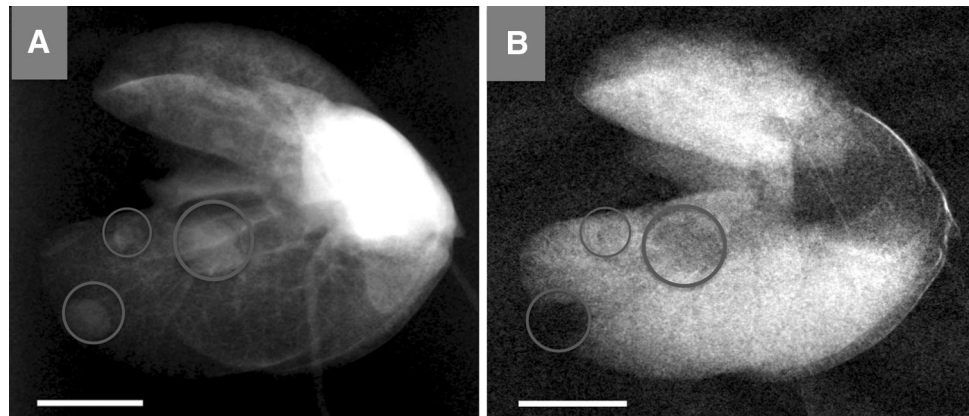
#### Pulmonary Nodules

Pulmonary nodules represent another pathology that is often challenging to detect on conventional chest radiographs. It has been demonstrated that the sensitivity of chest X-rays to detect lung cancers with a mean size of approximately 2 cm is in the range of only 50 % [31]. Since pulmonary nodules incidentally detected on chest X-ray may represent early lung cancer, the limited sensitivity of conventional chest radiographs for their

detection is problematic. A recent feasibility study, therefore, investigated whether grating-based multi-modal chest radiography may be of value for the detection of pulmonary nodules [32•]. The authors used an ex vivo murine lung bearing multiple tumors derived from a genetically modified mouse model. The study demonstrated that lung tumors are visible on all three imaging modalities that can be derived from grating-based radiography (Fig. 3). In the transmission image—which corresponds to a conventional chest radiograph—lung nodules were visible as sharply demarcated areas of decreased transmission due to the X-ray attenuation in the tumor. In the dark-field image, lung tumors appeared as areas of decreased scatter signal. This is due to the replacement of the highly scattering lung tissue with its multiple tissue-air interfaces by the rather homogenous soft tissue mass of the lung tumor. In the differential phase-contrast image, the tumors were characterized by the phase shift occurring at the edges of the nodule. However, in this initial study, no additional tumors were visible in the dark-field or phase-contrast images that had not been detected in the transmission image. The study thus did not find evidence for an increase in sensitivity by adding dark-field and phase-contrast imaging to conventional chest radiography.



**Fig. 3** Lung tumor imaging in ex vivo mouse lungs. Corresponding lung nodules in transmission (a) and dark-field (b) images [32•] are marked with gray circles



### Pneumothorax

A pneumothorax occurs when air enters into the pleural space leading to a partial or complete collapse of the lung on the affected side. On conventional chest radiographs, small pneumothoraces can easily be overlooked. Due to the low density of lung tissue, the difference in attenuation between air and lung is minimal. Frequently, the pneumothorax can only be recognized due to the absence of vascular markings and the fine pleural line separating lung and pneumothorax. On dark-field radiographs, the presence and extent of a pneumothorax can be easily recognized by the sharp contrast between the absent dark-field signal in the pneumothorax and the strong dark-field signal of the lung. Weber and colleagues have explored this potential application in their study, where bilateral pneumothoraces were incidentally detected in one of the mice imaged *post mortem* [21].

### Other Pulmonary Pathologies

To date, no other pulmonary pathologies have been investigated with grating-based dark-field radiography. Many other pulmonary pathologies such as pulmonary infections and fibrosing interstitial lung disease likely interfere with the scattering characteristics of the affected parenchyma and could thus be detected on dark-field chest radiographs. Whether or not dark-field radiography can provide a diagnostic benefit for the detection, and characterization of these pathologies remains to be investigated.

### Breast Imaging

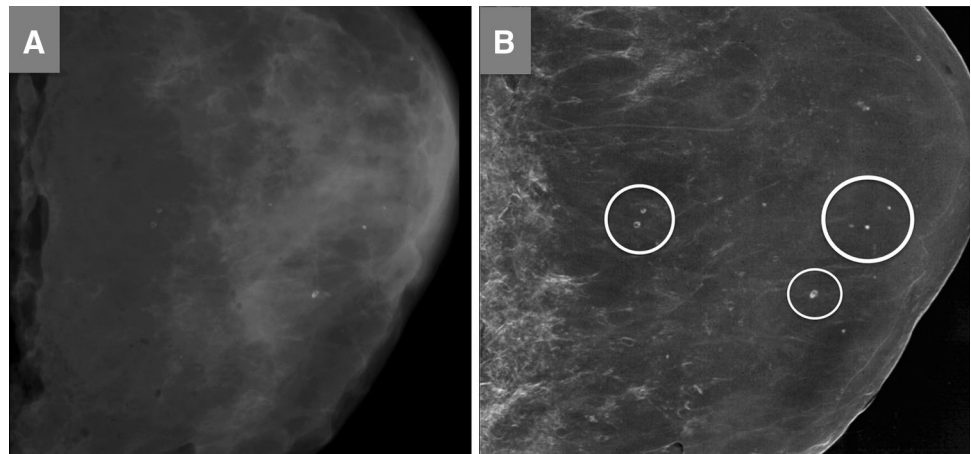
Mammography has been demonstrated to reduce breast cancer mortality [33] although the precise strength of this benefit and its relationship with potential harms of breast cancer screening such as overtreatment and psychological

distress remains controversial [34]. Nevertheless, annual or biennial mammography for breast cancer screening is generally recommended for women aged 50–69 years [35]. The detection of breast cancer on mammograms is challenging with a high rate of false-positive findings prompting unnecessary biopsies.

The breast is composed of soft tissue, which *per se* produces little small-angle X-ray scattering and thus does not immediately appear suitable for dark-field radiography. Indeed, phase-contrast (and not dark-field) radiography with its superior soft tissue contrast compared to conventional radiography has been the focus of interest in mammography and has even been assessed in clinical trials [36]. Dark-field mammography is a much more recent concept, and its potential is largely grounded in the association of breast cancer with micro-calcifications. It has been shown that 30–50 % of breast cancers demonstrate micro-calcifications on mammograms, and 60–80 % of breast cancers show micro-calcifications on histo-pathological examination [37]. The promise of dark-field mammography lies in the fact that micro-calcifications may be too small to be visible on conventional mammograms but cause X-ray scattering, which can be detected on dark-field imaging (Fig. 4).

Schleede and colleagues imaged a mammography phantom with grating-based imaging at a compact synchrotron light source and reported an increase in image contrast attainable through phase-contrast and dark-field imaging over conventional attenuation-based projections [38]. Stampanoni and colleagues first used grating-based radiography to image full-breast human mastectomy samples bearing breast cancers [39••]. They found that the phase-contrast and dark-field signal can be used to create color-coded fusion images that enhance tumor visibility. The authors subsequently determined the value of their approach in a larger study using fresh mastectomy samples from 33 patients and six breast radiologists as readers [40]. The results of this study suggested that the addition of

**Fig. 4** Ex vivo radiographs of human mastectomy sample. Absorption (a) and dark-field (b) images acquired in craniocaudal projection are shown. This mastectomy sample contains a ductal carcinoma in situ, which had been subtotally removed by a punch biopsy. Note that the dark-field image is more sensitive for the visualization of microcalcifications (*circles*) [50]



phase-contrast and dark-field information to absorption images improved the overall image sharpness, allowed for better delineation of breast lesions and increased the visibility of calcifications.

Anton and colleagues imaged human mastectomy samples and detected an area of increased dark-field signal, which corresponded to a tumor region containing small calcification grains [41]. A subsequent publication by the same research group confirmed that micro-calcifications with a grain size of 1–40  $\mu\text{m}$  were responsible for the changes in dark-field signal observed in dark-field breast radiography [42]. Interestingly, both tumors imaged in this study were invisible on conventional radiography, but one of them could be detected on the dark-field image due to the signal alterations from micro-calcifications within the tumor.

These findings may be clinically relevant, since ductal *carcinoma in situ* (a precursor lesion which may progress to invasive breast cancer) can often only be detected on mammography due to microcalcifications. However, no reliable data exist whether or not dark-field mammography can differentiate microcalcifications of benign and malignant etiology.

### Musculoskeletal Imaging

Several groups have made some effort to evaluate the benefit of dark-field radiography for bone imaging. The main advantage of x-ray dark-field imaging for bone applications is seen in the fact that dark-field imaging can reveal information about substructures of the bone that are not directly resolved on the transmission image. Thus, Wen and colleagues reported images of mineralized collagen fibrils and porosities of the mineralized matrix [16]. Further studies demonstrated that X-ray dark-field radiography can yield information about bone micro-architecture, without

the need to directly resolve the structures [43–45]. It was confirmed using high resolution CT scans that the directional dark-field signal originates from X-ray scattering on trabecular micro-architecture in bone. A further recent publication by Thüring and colleagues presented a radiograph of a human hand cadaver specimen [46] acquired with a grating-based setup. In their study, the dark-field image was visually rated as superior to the absorption image for the delineation of bone and the depiction of the joint spaces and provided superior visualization of periarticular soft tissue calcifications.

### Emerging Biomedical Applications

Based on the very promising results in lung imaging, it has been hypothesized that microbubbles, which are typically used as a contrast agent for ultrasound imaging, can be used to produce contrast in dark-field radiography. A first proof-of-principle study by Velroyen et al. [47] demonstrated that considerable signal can indeed be generated. However, further studies demonstrating similar results in situ and in vivo are needed to confirm the utility of microbubbles as contrast agents for dark-field radiography. This approach may allow for performing angiographic examinations without iodinated contrast agents.

### Challenges and Future Perspectives

#### Toward Dark-Field X-ray Tomography

Dark-field tomography can be performed very similar to the conventional absorption CT [48]. However, there is a significant difference in information that is obtained. Conventional X-ray transmission tomography yields the distribution of the linear attenuation coefficient, i.e., how

much radiation is locally absorbed by the sample. Similar to the attenuation coefficient of a material, a linear diffusion coefficient is introduced for dark-field imaging. The diffusion coefficient is a material dependent variable describing the specific scattering width (angle distribution) per unit length of the sample [48]. Thus, similar to the transmission CT, the dark-field tomography gives the distribution of the diffusion coefficient, i.e., the local scattering power. For example, a dark-field CT of the lung would not visualize lung density but rather the frequency of air/tissue interfaces as sources of small-angle X-ray scattering. This means that alveoli do not have to be directly resolved, to retrieve information about their size. However, dark-field tomography has not yet been performed in vivo, and it remains to be demonstrated whether it is feasible with a radiation dose and acquisition time suitable for the in vivo setting.

### Challenges for the Clinical Application of X-ray Dark-Field Imaging

X-ray dark-field imaging is still in the preclinical phase of development and has not been used in living humans. The transition of this technique for the clinical use in patients will require a number of further technical developments. First, the size of currently available gratings limits the field of view that can be imaged with a single acquisition. In the laboratory environment, larger specimens are often imaged by combining images derived from multiple acquisitions, but this requires acquisition times that are impractical for clinical use. Thus, larger gratings have to be developed to provide a field of view that is sufficient for clinical radiography applications. Second, the currently available technical equipment for grating-based X-ray imaging is still in a prototype stage. Therefore, the radiation dose associated with grating-based radiography is still substantially higher than would be acceptable for clinical use. Further technical developments will thus need to focus on optimizing the dose efficiency of grating-based X-ray imaging setups. As the third challenge, the preclinical studies on dark-field radiography have been performed with relatively low photon energies in the order of 20–40 keV. This photon energy may be compatible with clinical requirements for mammography, where only few centimeters of tissue need to be penetrated, and low photon energies are beneficial due to their higher soft tissue contrast [38]. However, for most other clinical applications, the technique will need to be adapted to considerably higher photon energies. This is certainly the case for lung imaging, where the X-ray beam has to penetrate the human chest. As the first step in this direction, the feasibility of X-ray phase-contrast imaging at 82 keV has recently been demonstrated [49].

### Conclusion

X-ray dark-field is an emerging imaging modality that has shown a high potential for substantially expanding the diagnostic information that can be gained from radiographs. During the past years, a number of applications have been identified that could benefit considerably from this new imaging modality. Among the most promising are lung imaging, mammography, and bone imaging. Even if the progress in the field of X-ray phase-contrast and dark-field imaging has recently been considerable, no studies have thus far been performed on living humans. Numerous technical challenges still have to be overcome before this imaging modality can be introduced into the clinical world.

**Acknowledgments** We acknowledge financial support through the DFG Cluster of Excellence Munich-Centre for Advanced Photonics (MAP), the DFG Gottfried Wilhelm Leibniz program, and the European Research Council (ERC, FP7, StG 240142). AY acknowledges the support of his studies through the TU München graduate school.

### Compliance with Ethics Guidelines

**Conflict of Interest** Dr. Andre Yaroshenko, Dr. Katharina Hellbach, Dr. Martin Bech, Dr. Susanne Grandl, Dr. Franz Pfeiffer, and Dr. Felix G. Meinel each declare no potential conflicts of interest. Dr. Maximilian F. Reiser reports personal fees from Ludwig-Maximilians-University of Munich, Germany, grants from German Research Society (DFG-Deutsche Forschungsgemeinschaft) “Cluster of Excellence”, grants from EUROBIOIMAGING, grants from German National Cohort, grants from Munich Cluster of Excellence—M4—Imaging, grants from BMBF German Center for Lung Diseases, grants from BMBF German Center for Cardiovascular Diseases, outside the submitted work.

**Human and Animal Rights and Informed Consent** This article does not contain any studies with human or animal subjects performed by any of the authors.

### References

Papers of particular interest, published recently, have been highlighted as

- Of importance
- Of major importance

1. Als-Nielsen J, McMorrow D. Elements of modern X-ray physics. México: Wiley; 2011.
2. Murphy DB. Fundamentals of light microscopy and electronic imaging. New York: Wiley; 2001.
3. Snigirev A, Snigireva I, Kohn V, Kuznetsov S, Schelokov I. On the possibilities of x-ray phase contrast microimaging by coherent high-energy synchrotron radiation. Rev Sci Instrum. 1995;66(12):5486–92.
4. Wilkins SW, Gureyev TE, Gao D, Pogany A, Stevenson AW. Phase-contrast imaging using polychromatic hard X-rays. Nature. 1996;384:335–7.

5. Cloetens P, Ludwig W, Baruchel J, et al. Holotomography: quantitative phase tomography with micrometer resolution using hard synchrotron radiation x rays. *Appl Phys Lett*. 1999;75(19):2912–4.
6. Davis TJ, Gao D, Gureyev TE, Stevenson AW, Wilkins SW. Phase-contrast imaging of weakly absorbing materials using hard x-rays. *Nature*. 1995;373:595–8.
7. Momose A, Kawamoto S, Koyama I, Hamaishi Y, Takai K, Suzuki Y. Demonstration of x-ray Talbot interferometry. *Jpn J Appl Phys*. 2003;42:866–8.
8. Bonse U, Hart M. An x-ray interferometer with long separated interfering beam paths. *Appl Phys Lett*. 1965;7(4):99–100.
9. Pfeiffer F, Weitkamp T, Bunk O, David C. Phase retrieval and differential phase-contrast imaging with low brilliance x-ray sources. *Nat Phys*. 2006;2:258–61.
10. Pfeiffer F, Bech M, Bunk O, et al. Hard x-ray dark-field imaging using a grating interferometer. *Nat Mater*. 2008;7:134–7.
11. Weitkamp T, Diaz A, David C, et al. X-ray phase imaging with a grating interferometer. *Opt Express*. 2005;13(16):6296–304.
12. Pfeiffer F, Bech M, Bunk O, et al. Hard-X-ray dark-field imaging using a grating interferometer. *Nat Mater*. 2008;7(2):134–7.
13. Thuring T, Modregger P, Pinzer BR, Wang Z, Stampanoni M. Non-linear regularized phase retrieval for unidirectional X-ray differential phase contrast radiography. *Opt Express*. 2011;19(25):25545–58.
14. Matías Di Martino J, Flores JL, Pfeiffer F, Scherer K, Ayubi GA, Ferrari JA. Phase retrieval from one partial derivative. *Opt Lett*. 2013;38(22):4813–6.
15. Wen H, Bennett EE, Hegedus MM, Carroll SC. Spatial harmonic imaging of x-ray scattering—initial results. *IEEE Trans Med Imaging*. 2008;27(8):997–1002.
16. Wen H, Bennett EE, Hegedus MM, Rapacchi S. Fourier X-ray scattering radiography yields bone structural information. *Radiology*. 2009;251(3):910–8.
17. • Momose A, Yashiro W, Harase S, Kuwabara H. Four-dimensional X-ray phase tomography with Talbot interferometry and white synchrotron radiation: dynamic observation of a living worm. *Opt Express*. 2011;19(9):8423–8432. This publication demonstrates the feasibility to acquire phase information with very short exposure times.
18. Bevins N, Zambelli J, Li K, Qi Z, Chen G-H. Multicontrast x-ray computed tomography imaging using Talbot-Lau interferometry without phase stepping. *Med Phys*. 2011;39(1):424–8.
19. •• Schleede S, Meinel FG, Bech M, et al. Emphysema diagnosis using X-ray dark-field imaging at a laser-driven compact synchrotron light source. *Proc Natl Acad Sci USA*. 2012;109(44):17880–17885. This publication demonstrated for the first time that grating-based X-ray imaging can be used to detect pulmonary emphysema and map its regional distribution on radiographs.
20. Schwab F, Schleede S, Hahn D, et al. Comparison of contrast-to-noise ratios of transmission and dark-field signal in grating-based X-ray imaging for healthy murine lung tissue. *Z Med Phys*. 2013;23(3):236–42.
21. Weber T, Bayer F, Haas W, et al. Investigation of the signature of lung tissue in X-ray grating-based phase-contrast imaging. 2012. <https://archive.org/details/arxiv-1212.5031>. Accessed 5 Jan 2014.
22. •• Bech M, Tapfer A, Velroyen A, et al. In-vivo dark-field and phase-contrast x-ray imaging. *Sci Rep*. 2013;3:3209. This was the first study to perform grating-based dark-field radiography in vivo.
23. Miniati M, Monti S, Stolk J, et al. Value of chest radiography in phenotyping chronic obstructive pulmonary disease. *The Eur Respir J: Off J Eur Soc Clin Respir Physiol*. 2008;31(3):509–15.
24. Thurlbeck WM, Simon G. Radiographic appearance of the chest in emphysema. *Am J Roentgenol (AJR)*. 1978;130(3):429–40.
25. Washko GR. Diagnostic imaging in COPD. *Semin Respir Crit Care Med*. 2010;31(3):276–85.
26. Muller NL, Coxson H. Chronic obstructive pulmonary disease. 4: imaging the lungs in patients with chronic obstructive pulmonary disease. *Thorax*. 2002;57(11):982–5.
27. • Meinel FG, Schwab F, Schleede S, et al. Diagnosing and mapping pulmonary emphysema on X-ray projection images: incremental value of grating-based X-ray dark-field imaging. *PLoS One*. 2013;8(3):e59526. This analysis demonstrated for the first time that grating-based dark-field radiography is superior to conventional radiography for the detection of pulmonary emphysema and the assessment of its regional distribution.
28. •• Yaroshenko A, Meinel FG, Bech M, et al. Pulmonary emphysema diagnosis with a preclinical small-animal X-ray dark-field scatter-contrast scanner. *Radiology*. 2013;269(2):427–433. This publication demonstrated that dark-field radiography for pulmonary emphysema diagnosis can be performed using a conventional polychromatic X-ray source.
29. Tapfer A, Bech M, Velroyen A, et al. Experimental results from a preclinical X-ray phase-contrast CT scanner. *Proc Natl Acad Sci USA*. 2012;109(39):15691–6.
30. •• Meinel FG, Yaroshenko A, Hellbach K, et al. Improved diagnosis of pulmonary emphysema using in vivo dark-field radiography. *Invest Radiol*. 2014;49. This study demonstrated for the first time that dark-field radiography can detect pulmonary emphysema in vivo.
31. Freedman MT, Lo SC, Seibel JC, Bromley CM. Lung nodules: improved detection with software that suppresses the rib and clavicle on chest radiographs. *Radiology*. 2011;260(1):265–73.
32. • Meinel FG, Schwab F, Yaroshenko A, et al. Lung tumors on multimodal radiographs derived from grating-based X-ray imaging—A feasibility study. *Phys Med*. 2013;30(3):352–357. First report on imaging pulmonary nodules with grating-based phase-contrast and dark-field radiography.
33. Nelson HD, Tyne K, Naik A, et al. Screening for breast cancer: an update for the U.S. preventive services task force. *Ann Intern Med*. 2009;151(10):727–737, W237–742.
34. Gotzsche PC, Jorgensen KJ. Screening for breast cancer with mammography. *Cochrane Database Syst Rev*. 2013;6:CD001877.
35. Warner E. Clinical practice. Breast-cancer screening. *N Engl J Med*. 2011;365(11):1025–32.
36. Castelli E, Tonutti M, Arfelli F, et al. Mammography with synchrotron radiation: first clinical experience with phase-detection technique. *Radiology*. 2011;259(3):684–94.
37. Sakka E, Prentza A, Koutsouris D. Classification algorithms for microcalcifications in mammograms (Review). *Oncol Rep*. 2006;15:1049–55.
38. Schleede S, Bech M, Achterhold K, et al. Multimodal hard X-ray imaging of a mammography phantom at a compact synchrotron light source. *J Synchrotron Radiat*. 2012;19(Pt 4):525–9.
39. •• Stampanoni M, Wang Z, Thuring T, et al. The first analysis and clinical evaluation of native breast tissue using differential phase-contrast mammography. *Invest Radiol*. 2011;46(12):801–806. Study demonstrating the incremental diagnostic value of phase-contrast and dark-field imaging in mammography.
40. Hauser N, Wang Z, Kubik-Huch RA, et al. A study on mastectomy samples to evaluate breast imaging quality and potential clinical relevance of differential phase contrast mammography. *Invest Radiol*. 2013;49(3):131–7.
41. Anton G, Bayer F, Beckmann MW, et al. Grating-based darkfield imaging of human breast tissue. *Z Med Phys*. 2013;23(3):228–35.
42. Michel T, Rieger J, Anton G, et al. On a dark-field signal generated by micrometer-sized calcifications in phase-contrast mammography. *Phys Med Biol*. 2013;58(8):2713–32.



43. Potdevin G, Malecki A, Biernath T, et al. X-ray vector radiography for bone micro-architecture diagnostics. *Phys Med Biol.* 2012;57(11):3451–61.
44. Schaff F, Malecki A, Potdevin G, et al. Correlation of x-ray vector radiography to bone micro-architecture. *Nat Sci Rep.* 2013;3694:3695.
45. Guillaume P, Andreas M, Thomas B, et al. X-ray vector radiography for bone micro-architecture diagnostics. *Phys Med Biol.* 2012;57(11):3451.
46. Thuring T, Guggenberger R, Alkadhi H, et al. Human hand radiography using X-ray differential phase contrast combined with dark-field imaging. *Skelet Radiol.* 2013;42(6):827–35.
47. Velroyen A, Bech M, Malecki A, et al. Microbubbles as a scattering contrast agent for grating-based x-ray dark-field imaging. *Phys Med Biol.* 2013;58(4):N37.
48. Bech M, Bunk O, Donath T, Feidenhans'l R, David C, Pfeiffer F. Quantitative x-ray dark-field computed tomography. *Phys Med Biol.* 2010;55(18):5529.
49. • Willner M, Bech M, Herzen J, et al. Quantitative X-ray phase-contrast computed tomography at 82 keV. *Opt Express.* 2013;21(4):4155–4166. Study demonstrating the feasibility of phase-contrast and dark-field imaging at clinically relevant energies.
50. Auweter SD, Herzen J, Willner M, et al. X-ray phase-contrast imaging of the breast—advances towards clinical implementation. *Br J Radiol.* 2014;87(1034):20130606.